THE JOURNAL OF PHYSICAL CHEMISTRY Letters

Letter

pubs.acs.org/JPCL

Large Enhancement in the Heterogeneous Oxidation Rate of Organic Aerosols by Hydroxyl Radicals in the Presence of Nitric Oxide

Nicole K. Richards-Henderson,[†] Allen H. Goldstein,[‡] and Kevin R. Wilson*[,†]

[†]Chemical Sciences Division, Lawrence Berkeley National Laboratory, Berkeley, California 94720, United States

[‡]Department of Environmental Science, Policy and Management, University of California Berkeley, Berkeley, California 94720, United States

Supporting Information

ABSTRACT: In the troposphere, the heterogeneous lifetime of an organic molecule in an aerosol exposed to hydroxyl radicals (OH) is thought to be weeks, which is orders of magnitude slower than the analogous gas phase reactions (hours). Here, we report an unexpectedly large acceleration in the effective heterogeneous OH reaction rate in the presence of NO. This 10−50 fold acceleration originates from free radical chain reactions, propagated by alkoxy radicals that form inside the aerosol by the reaction of NO with peroxy radicals, which do not appear to produce chain terminating products (e.g., alkyl nitrates), unlike gas phase mechanisms. A kinetic model, constrained by experiments, suggests that in polluted regions heterogeneous oxidation plays a much more prominent role in the daily chemical evolution of organic aerosol than previously believed.

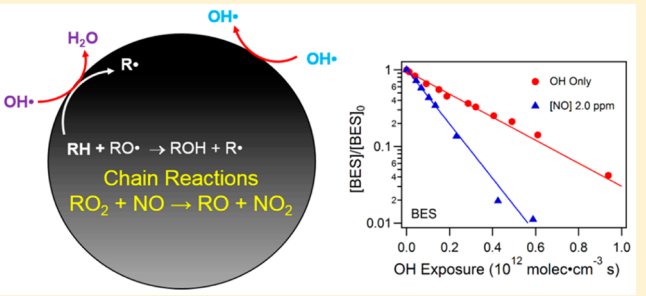

Organic material comprises a significant fraction of submicron tropospheric aerosol (20−90%).[1,2] Organic aerosol (OA), once formed or emitted into the atmosphere, is transformed by photochemical reactions, heterogeneous oxidation, aqueous phase chemistry, and the condensation of low-volatility organic species from the gas phase. These chemical transformations alter key microphysical OA properties (e.g., particle size, optical properties, volatility, toxicity, hygroscopicity) that in turn have large scale impacts on cloud droplet formation, human health, and radiative forcing.[3] For chemical transport models to accurately predict the impact that OA has on air quality and climate relies on accurate descriptions of multiphase chemistry and their associated kinetic time scales.[4] Secondary organic aerosol (SOA) formation is fast and occurs within hours by reactions of O_3 and OH with gas phase anthropogenic and biogenic SOA precursors. Heterogeneous aerosol oxidation is generally considered to be at least ∼10 times slower (i.e., weeks), occurring on a similar time scale as dry and wet deposition. Here, new experimental evidence is reported for radical chain reactions initiated by a heterogeneous reaction in the presence of two common anthropogenic pollutants. This free radical chain reaction leads to large effective reaction rates and much shorter kinetic lifetimes (hours) than previously thought possible for heterogeneous oxidation.

Scheme 1 shows a canonical reaction mechanism used to explain the heterogeneous OH oxidation of hydrocarbons (RH) in the presence of O_2. OH reacts with RH by H atom abstraction forming an alkyl radical (R) and H_2O. The heterogeneous rate of the reaction is quantified by a reactive uptake coefficient (γ), which is determined by measuring the loss of either gas-phase OH or particle phase RH. Kinetic measurements of OH loss by definition yield $\gamma_{OH} \leq 1$. This is not necessarily the case when the reaction is measured by the decay of RH because, in addition to OH, other free radical intermediates (i.e., RO, Scheme 1) can consume the hydrocarbon leading to effective uptake coefficients (γ_{eff}) larger than 1. $\gamma_{eff} > 1$ simply means that the reactive decay of the hydrocarbon includes secondary chemistry.

Once formed, the alkyl radical (R) quickly reacts in the atmosphere with O_2 to produce a peroxy radical (RO_2). Peroxy radicals are relatively slow to react and can diffuse over much larger distances within the aerosol than either OH or R. In the absence of NO_x, RO_2 reacts primarily with another RO_2 to form either a carbonyl−alcohol pair or two alkoxy radicals (RO). RO, if formed, is significantly more reactive than RO_2 and, for instance, can abstract a H atom (chain propagation) from a neighboring molecule to form another R and subsequently another RO_2.[5] This and many other laboratories report that $0.1 \leq \gamma_{eff} \leq 1$, suggesting that in the atmosphere, heterogeneous oxidation is slow and only important for oxidative aging at longer time scales (weeks to months).[6] This also indicates that in the particle phase the branching ratio to form RO from the $RO_2 + RO_2$ reaction is small, producing instead mainly stable chain termination reaction products.

Received: September 23, 2015
Accepted: October 27, 2015

DOI: 10.1021/acs.jpclett.5b02121
J. Phys. Chem. Lett. 2015, 6, 4451−4455

Scheme 1. Generalized Reaction Scheme for the Oxidation of Saturated Hydrocarbons by OH in the Presence of NO_x

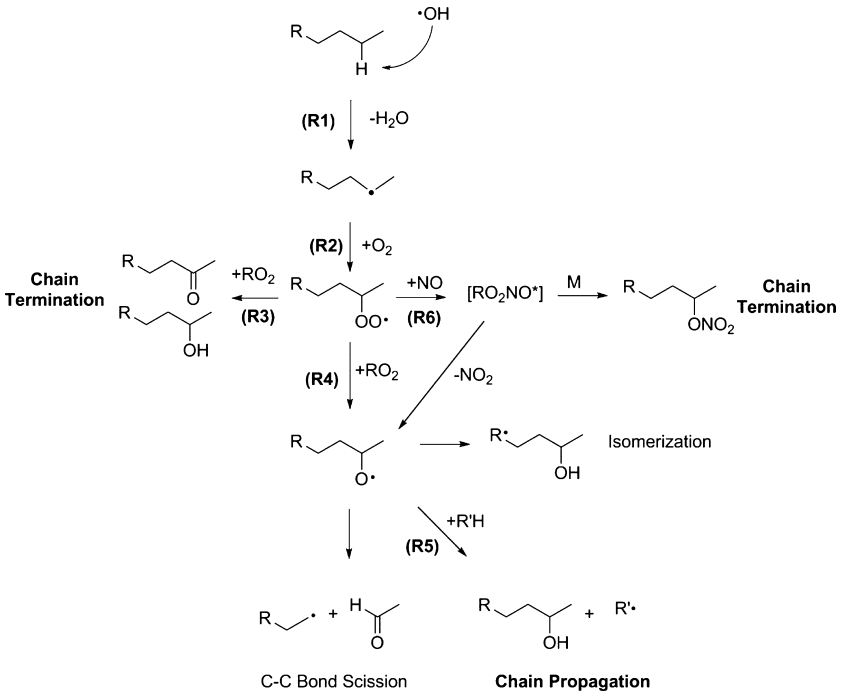

In polluted atmospheres, NO_x ($NO + NO_2$) is emitted from fossil fuel combustion with atmospheric mixing ratios as high as 200 ppb.[7−10] RO_2 radicals have been shown to readily oxidize nitric oxide (NO) both in the gas and aqueous-phase resulting in the formation of RO (and NO_2) and organic nitrates ($RONO_2$).[11−13] To examine how NO controls γ_{eff}, heterogeneous OH reactions were measured on three organic aerosol proxies: squalane (Sq, $C_{30}H_{62}$, liquid), bis(2-ethylhexyl) sebacate (BES, $C_{26}H_{50}O_4$, liquid), and triacontane (Tri, $C_{30}H_{62}$, solid). Kinetic measurements (described in the Supporting Information section 1 and 2), used to determine γ_{eff}, are conducted over a large range of concentrations: $\sim 6 \times 10^6 \leq [OH] \leq \sim 1 \times 10^{10}$ molecules cm^{-3}, 40 ppb $\leq [NO] \leq 2$ ppm (residence time of 37 s to hours).[14,15]

Figure 1a−c shows γ_{eff} as a function of $[NO_x]$ for the three proxy organic aerosols at two average $[OH]_{avg}$: 1×10^8 and 1×10^{10} molecules cm^{-3}. For all of the aerosols, γ_{eff} exhibits a clear increase as a function of $[NO_x]$. At $[OH] = 1 \times 10^{10}$ molecules cm^{-3} and NO_x = 250 ppb, the γ_{eff} is 0.45, 0.88, and 0.19 for Sq, BES, and Tri, respectively, whereas at NO_x = 2 ppm, the γ_{eff} is increased to 1.1, 1.7, and 0.3 for Sq, BES, and Tri, respectively. At $[OH] = 1 \times 10^8$ molecules cm^{-3}, the increase in γ_{eff} is much more pronounced. For example, at $[NO_x] = \sim 50$ ppb the γ_{eff} is 0.77, 1.7, 0.37 for Sq, BES, and Tri, respectively, and at NO_x = 150 ppb the γ_{eff} is 1.6, 3.9, and 0.6 for Sq, BES, and Tri, respectively. Values of $\gamma_{eff} > 1$ indicate that Sq and BES are consumed faster than the collision rate of OH with the aerosol particles, providing clear evidence of radical chain propagation chemistry within the particle. At all [OH], solid Tri particles exhibit a similar trend as the liquid particles, although overall increase in γ_{eff} is much slower due to diffusive limitations.[16,17] Although NO_2 is formed in the reactors, we conducted experiments with NO_2 only and found no discernible enhancement in the rate relative to the OH-only case (see Supporting Information section 3), suggesting that NO, rather than NO_2, is accelerating the reaction.

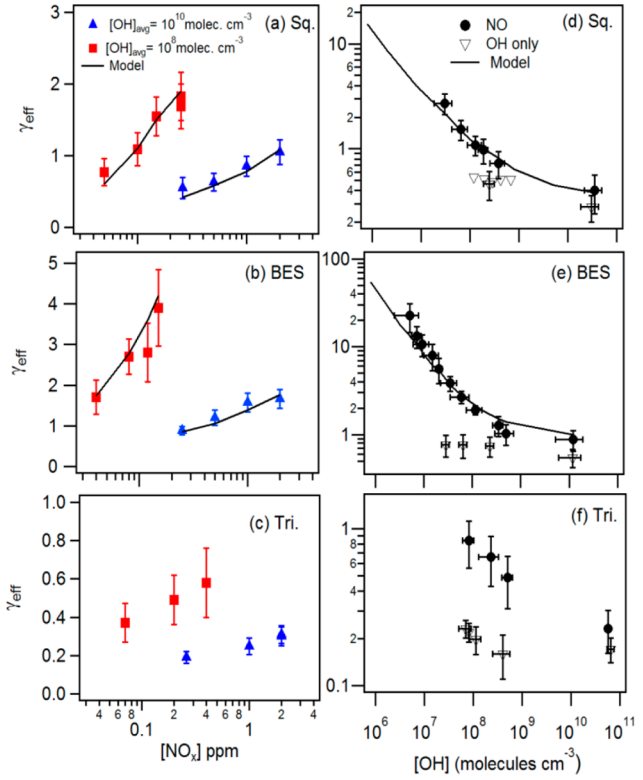

Figure 1. γ_{eff} as a function of $[NO_x]$ for (a) Sq, (b) BES, and (c) Tri. The symbols are for $[OH]_{avg} = 10^{10}$ molecules cm^{-3} (red squares) and 10^8 molecules cm^{-3} (blue triangles). γ_{eff} at as a function of [OH] with $[NO_x]$ = 84 ± 22 ppb (black circles) or without NO (black open triangles) for: (d) Sq, (e) BES, and (f) Tri. The lines are model predictions. Error bars represent ±1 SE (standard error) propagated from the standard errors of k_{Hex}, k_{eff}, and particle diameter.

In addition to [NO], absolute [OH] plays a significant role in determining the overall rate of the heterogeneous reaction.

DOI: 10.1021/acs.jpclett.5b02121
J. Phys. Chem. Lett. 2015, 6, 4451−4455

Table 1. Reaction Scheme and Rate Constants for Stochastic Simulations

number[a]	reaction	k	comment/ref
R1	$RH(n) + OH \rightarrow R(n) + H_2O$ (n = 0–4)		[b]
R2	$R(n) + O_2 \rightarrow ROO(n)$ (n = 0–4)	6.23×10^{6}	5[c]
R3	$ROO(n) + ROO(m) \rightarrow RH(n+1) + RH(m+1)$ (n,m = 0–4)	4.00×10^{-15}	5
R4	$2\ ROO(n) \rightarrow 2\ RO(n)$	1.00×10^{-16}	5
R5	$RH + RO(n) \rightarrow R(n+1) + R(n)$	1.66×10^{-15}	5
R6	$ROO(n) + NO \rightarrow RO(n) + NO_2$	6.5×10^{-12}	[d]

[a]A reaction diagram of this table is shown in Schematic 1. The letters n and m denote the number of oxygenated functional groups added to the squalane carbon backbone to form ketones or alcohols. [b]Treated as pseudo-first-order, where the average [OH] varies depending on experiment and k is from the experiment without added NO. Squalane, for example, has a k[OH] = 0.122, where k is 1.39×10^{-12} cm^3 molec^{-1} s^{-1} (γ = 0.27, d = 162 nm) and $[OH^{\bullet}]_{avg} = 9.5 \times 10^{10}$ molecules cm^{-3}.[15] [c]Treated as pseudo first order where [O_2] = 10%, $k = 2.5 \times 10^{-12}$ and the dimensionless Henry's law constant is 0.18. [d]The ROO + NO rate constant of 6.5×10^{-12} cm^3 molec^{-1} s^{-1} was determined by varying the pseudo-first-order rate constant (k[NO]) in order to match experimental data. The NO concentration in the particle phase was estimated using the unit less Henry's law constant, which is 8.2 ± 2.8,[20] and the NO concentration in the reactor. Model determined rate constant for ROO + NO are close to previously measured values ranging from $(2–5) \times 10^{-12}$ cm^3 molec^{-1} s^{-1}.[12,22]

This dependence is shown explicitly in Figure 1d–f at [NO] = 84 ± 22 ppb. As [OH] decreases from 10^{10} to 10^{7} molecule cm^{-3}, there is a steep increase in γ_{eff} (note the logarithmic scales). For Sq at [OH] = 3×10^{7} molecules cm^{-3}, γ_{eff} = 2.7, which is ∼10× faster than observed at 10^{10} molecules cm^{-3}. For BES, γ_{eff} = 23 at [OH] = 3×10^{6} molecules cm^{-3}, which is 26 times faster than observed at [OH] = 10^{10} molecules cm^{-3}. For Tri, γ_{eff} increases from 0.19 at [OH] = 1×10^{11} molecules cm^{-3} to near 1 at [OH] = 8×10^{7} molecules cm^{-3}. Also shown in Figure 1d–f are values for γ_{eff} measured in the absence of NO, which exhibit no strong dependence on [OH] and for all conditions remain less than 1. Several experiments were conducted to determine if O_3 (the OH precursor) or photochemistry were contributing to the large γ_{eff} observed in Figure 2 (Supporting Information section 4). Instead of O_3, H_2O_2 was used as the OH precursor and there was no discernible difference in the γ_{eff} at the same [OH] and [NO_x]. Measurements were also conducted using 355 nm lamps instead of 254 nm lamps to determine if photochemistry played a possible role, and again, there was no difference in the γ_{eff} or in product formation.

A kinetic model (Supporting Information section 5) of R1–R6 (Scheme 1) is formulated to elucidate the underlying reaction mechanism for the large enhancement in γ_{eff} with NO. Rate coefficients are from previous literature and are shown in Table 1.[5,18] The branching ratios, for the RO_2 self-reaction (R3) and (R4) to form either a carbonyl-alcohol pair (90%) or two RO (10%) are based upon a previous study.[19] Monodisperse aerosol size measurements, in which the surface-to-volume ratio of the particles was varied (Supporting Information section 6) indicate that the RO_2 + NO reaction occurs within the bulk of the aerosol and not at its surface. Thus, in the model, the [NO] in the particle phase is fixed by a unitless Henry's law constant of 8.2 ± 2.8 consistent with previous measurements.[20,21] Finally, after extensive efforts (documented in the Supporting Information section 7) failed to either detect any $RONO_2$ species or that they were formed but photolyzed in our reactor, we assume, unlike the gas phase, that the RO_2 + NO branching ratio to form RO is unity.

The only adjustable model parameter is the RO_2 + NO rate constant (R6). Previous literature constrains this to be on the order of 10^{-12} cm^3 molec^{-1} s^{-1}.[11,12] With this constraint, the model RO_2 + NO rate constant was varied to replicate the global data set (i.e., γ_{eff} vs [OH] and [NO]) as shown in Figure 1). Modeled and observed γ_{eff} match well for Sq and BES, using a RO_2 + NO rate constant of $6.5 \pm 3.2 \times 10^{-12}$ cm^3 molec^{-1} s^{-1}; consistent with previous literature ($2–5 \times 10^{-12}$ cm^3 molec^{-1} s^{-1}).[11,12] Tri particles were not modeled here because to accurately describe heterogeneous reactions in solid particles requires a spatially resolved reaction-diffusion model.

The model reveals that the relationship between γ_{eff}, [OH] and [NO] is controlled by the competition between free radical chain propagation (RO_2 + NO) and termination (RO_2 + RO_2). The competition is clearly illustrated in Figure 1, which shows γ_{eff} vs [OH] at 84 ± 22 ppb NO for each of the proxies. At high OH ($10^{8}–10^{10}$ molecules cm^{-3}), the concentration of RO_2 is also relatively high, so that the loss of RO_2 is dominated by reactions with other RO_2 to form stable chain terminating products. This also explains why a much higher [NO] is required at [OH] = 10^{10} molecules cm^{-3} than [OH] = 10^{8} molecules cm^{-3} to achieve the same γ_{eff} (e.g., [NO] = 2 ppm vs 100 ppb). At much lower [OH] approaching atmospheric levels ($10^{6}–10^{7}$ molecules cm^{-3}), RO_2 reacts primarily with NO to form RO, which chain propagate by H abstraction from a neighboring molecules to form R. This R reacts rapidly with O_2 to form another RO_2, which again reacts with NO to generate another RO (and so on), thereby propagating a radical chain reaction and increasing γ_{eff}. The kinetic model, constrained by measurements, predicts a drastic acceleration in chain propagation chemistry in polluted atmospheric conditions. In megacities,[7–10] for example, we predict that γ_{eff} (i.e., BES) at the lowest [OH] (8×10^{5} molecules cm^{-3}, [NO] = 85 ppb) is 55.2 and 0.8 in the presence of NO and without added NO, respectively.

A simple time scale analysis of these results suggests significant new implications for the short time evolution of OA by heterogeneous oxidation (with NO) in polluted regions. The heterogeneous lifetime of an alkane (i.e., squalane) in a 150 nm diameter particle with a γ_{eff} of 0.3 in a remote region (i.e., low NO_x) is four days, assuming a global mean [OH] of 2×10^{6} molecules cm^3. Under these same conditions, the lifetime of a gas-phase alkane (e.g., dodecane, $C_{12}H_{26}$) whose bimolecular rate constant is $k = 1.32 \times 10^{-11}$ cm^3 molecules^{-1} s^{-1} is 11 h. This large difference in gas vs heterogeneous lifetime (without NO added) is because particle phase molecules remain "hidden" inside the interior of the aerosol during most of their atmospheric lifetime and, therefore, unavailable for a surface reaction with OH. As shown here, the presence of free radical chain reactions initiated by OH at the surface, travel throughout the interior of the particle and accelerate oxidation rates by 10 to 50 times the OH collision frequency. Thus, we predict that in polluted environments,

DOI: 10.1021/acs.jpclett.5b02121
J. Phys. Chem. Lett. 2015, 6, 4451–4455

such as megacities, where NO concentrations are ~84 ppb and γ_{eff} = 9 (e.g., squalane) the heterogeneous lifetime is as short as ~3 h. Even at much lower [NO] (20 ppb, refer to Supporting Information section 8 for atmospheric conditions) but still significantly higher than pristine environments, γ_{eff} is predicted to be 3, yielding a heterogeneous oxidative lifetime of 10 h; comparable to the gas phase lifetime of dodecane. Therefore, in highly polluted regions, such as polluted urban centers, this chemistry could significantly accelerate the oxidative aging of OA.

Although these experiments use simple single component OA proxies that clearly do not reflect the immense complexity of real ambient aerosols, the free-radical chain propagation mechanism is general and expected to be relevant for the class of chemically reduced compounds (e.g., diesel emissions) commonly measured in primary urban OA.[23] Furthermore, the chain propagation pathway is based upon a well-established mechanism in the gas phase, but unlike the gas phase, the RO_2 + NO reaction in the organic aerosol phase appears to produce little if any chain termination products ($RONO_2$). In the condensed phase for large hydrocarbons, we would expect that the formation of organic nitrates to be in fact favored due to the solvent cage efficiently removing energy from the RO_2NO* intermediate.[24] However, it is possible that RO_2NO* in the condensed organic phase is stabilized but then decomposes into RO and NO_2. This reaction would be analogous to peroxynitrous acid (HOONO), which has a lifetime of seconds in water and decomposes to form NO_2 and OH.[25] For more highly oxygenated aerosols, the mechanism observed here is undoubtedly more complex because reaction with NO will produce activated alkoxy radicals with unimolecular decomposition (also chain propagating) rates that are competitive with bimolecular intermolecular H abstraction.[19]

These results provide new evidence that in polluted regions, heterogeneously initiated oxidation by OH can in fact contribute to the short time (hourly) chemical evolution of OA and, therefore, should be included in chemical transport models. Furthermore, heterogeneous oxidation (with chain propagation), unlike SOA formation, oxidizes the aerosol with a minimal increase in aerosol mass, which may explain why some atmospheric models often correctly predict aerosol mass loadings but under predict its degree of oxygenation (i.e., oxygen-to-carbon ratios).[26,27]

EXPERIMENTAL METHOD

Organic aerosol oxidation in the presence of NO was investigated by measuring the OH oxidation kinetics of three organic compounds: squalane ($C_{30}H_{62}$, liquid), bis(2-ethylhexyl) sebacate ($C_{26}H_{50}O_4$, liquid), or triacontane ($C_{30}H_{62}$, solid). Kinetic measurements were made in either a flow-tube reactor or a continuous-flow stir tank reactor (CFSTR), both are described in detail elsewhere,[14,15] using a vacuum ultraviolet (VUV) photoionization aerosol mass spectrometer (Supporting Information section 1). A description of the kinetic analysis conducted is provided in Supporting Information section 2.

Modeling was conducted using Kinetiscope (http://www.hinsberg.net/kinetiscope/), which uses stochastic algorithms (Supporting Information section 5) for chemical kinetics and was recently used for aerosol chemistry.[18,19] The kinetic model of R1−R6 (Figure 1) was formulated to elucidate the underlying reaction mechanism. Rate coefficients are from previous literature and are shown in Table 1.[5,18] The branching ratios for the RO_2 self-reactions (R3) and (R4) to form either a carbonyl−alcohol pair or two $RO^{\bullet}$ are fixed at 10:90, respectively, and based upon a previous study.[19]

ASSOCIATED CONTENT

Supporting Information

The Supporting Information is available free of charge on the ACS Publications website at DOI: 10.1021/acs.jpclett.5b02121.

Detailed description of experiment and model. (PDF)

AUTHOR INFORMATION

Corresponding Author

*E-mail: krwilson@lbl.gov.

Notes

The authors declare no competing financial interest.

ACKNOWLEDGMENTS

This work and the Advanced Light Source is supported by the Director, Office of Energy Research, Office of Basic Energy Science of the U.S. Department of Energy under Contract No. DE-AC02-05CH11231. K.R.W. is supported by the Department of Energy, Office of Science Early Career Research Program. We thank Dr. Frances Houle and Dr. Aaron Wiegel for technical support on the model, Dr. Michael Ward for assistance with experimental measurements and Mr. Bruce Rude for technical support on the instrument.

REFERENCES

(1) Zhang, Q.; Jimenez, J. L.; Canagaratna, M. R.; Allan, J. D.; Coe, H.; Ulbrich, I.; Alfarra, M. R.; Takami, A.; Middlebrook, A. M.; Sun, Y. L.; et al. Ubiquity and Dominance of Oxygenated Species in Organic Aerosols in Anthropogenically-Influenced Northern Hemisphere Midlatitudes. *Geophys. Res. Lett.* **2007**, *34*, L13801.

(2) Murphy, D. M.; Cziczo, D. J.; Froyd, K. D.; Hudson, P. K.; Matthew, B. M.; Middlebrook, A. M.; Peltier, R. E.; Sullivan, A.; Thomson, D. S.; Weber, R. J. Single-Particle Mass Spectrometry of Tropospheric Aerosol Particles. *J. Geophys. Res.* **2006**, *111*, D23S32.

(3) Pöschl, U. Atmospheric Aerosols: Composition, Transformation, Climate and Health Effects. *Angew. Chem., Int. Ed.* **2005**, *44*, 7520−7540.

(4) Jimenez, J. L.; Canagaratna, M. R.; Donahue, N. M.; Prevot, A. S. H.; Zhang, Q.; Kroll, J. H.; DeCarlo, P. F.; Allan, J. D.; Coe, H.; Ng, N. L.; et al. Evolution of Organic Aerosols in the Atmosphere. *Science* **2009**, *326*, 1525−1529.

(5) Denisov, E. T.; Afanas'ev, I. B. *Oxidation and Antioxidants in Organic Chemistry and Biology*; Taylor & Frances: Boca Raton, FL, 2005.

(6) George, I. J.; Abbatt, J. P. D. Heterogeneous Oxidation of Atmospheric Aerosol Particles by Gas-Phase Radicals. *Nat. Chem.* **2010**, *2*, 713−722.

(7) Qin, Y.; Tonnesen, G. S.; Wang, Z. Weekend/Weekday Differences of Ozone, NOx, CO, VOCs, PM10 and the Light Scatter During Ozone Season in Southern California. *Atmos. Environ.* **2004**, *38*, 3069−3087.

(8) Khoder, M. I. Diurnal, Seasonal and Weekdays−Weekends Variations of Ground Level Ozone Concentrations in an Urban Area in Greater Cairo. *Environ. Monit. Assess.* **2009**, *149*, 349−362.

(9) Stephens, S.; Madronich, S.; Wu, F.; Olson, J. B.; Ramos, R.; Retama, A.; Muñoz, R. Weekly Patterns of México City's Surface Concentrations of Co, Nox, Pm10 and O3 During 1986−2007. *Atmos. Chem. Phys.* **2008**, *8*, 5313−5325.

(10) Molina, M. J.; Molina, L. T. Megacities and Atmospheric Pollution. *J. Air Waste Manage. Assoc.* **2004**, *54*, 644−680.

(11) Goldstein, S.; Lind, J.; Merenyi, G. Reaction of Organic Peroxyl Radicals with •No2 and •No in Aqueous Solution: Intermediacy of

DOI: 10.1021/acs.jpclett.5b02121
J. Phys. Chem. Lett. 2015, 6, 4451−4455

Organic Peroxynitrate and Peroxynitrite Species. *J. Phys. Chem. A* **2004**, *108*, 1719−1725.
(12) Padmaja, S.; Huie, R. E. The Reaction of Nitric Oxide with Organic Peroxyl Radicals. *Biochem. Biophys. Res. Commun.* **1993**, *195*, 539−544.
(13) Eberhard, J.; Howard, C. J. Rate Coefficients for the Reactions of Some C3 to C5 Hydrocarbon Peroxy Radicals with No. *J. Phys. Chem. A* **1997**, *101*, 3360−3366.
(14) Che, D. L.; Smith, J. D.; Leone, S. R.; Ahmed, M.; Wilson, K. R. Quantifying the Reactive Uptake of Oh by Organic Aerosols in a Continuous Flow Stirred Tank Reactor. *Phys. Chem. Chem. Phys.* **2009**, *11*, 7885−7895.
(15) Smith, J. D.; Kroll, J. H.; Cappa, C. D.; Che, D. L.; Liu, C. L.; Ahmed, M.; Leone, S. R.; Worsnop, D. R.; Wilson, K. R. The Heterogeneous Reaction of Hydroxyl Radicals with Sub-Micron Squalane Particles: A Model System for Understanding the Oxidative Aging of Ambient Aerosols. *Atmos. Chem. Phys.* **2009**, *9*, 3209−3222.
(16) Ruehl, C. R.; Nah, T.; Isaacman, G.; Worton, D. R.; Chan, A. W. H.; Kolesar, K. R.; Cappa, C. D.; Goldstein, A. H.; Wilson, K. R. The Influence of Molecular Structure and Aerosol Phase on the Heterogeneous Oxidation of Normal and Branched Alkanes by Oh. *J. Phys. Chem. A* **2013**, *117*, 3990−4000.
(17) Renbaum, L. H.; Smith, G. D. The Importance of Phase in the Radical-Initiated Oxidation of Model Organic Aerosols: Reactions of Solid and Liquid Brassidic Acid Particles. *Phys. Chem. Chem. Phys.* **2009**, *11*, 2441−2451.
(18) Houle, F. A.; Hinsberg, W. D.; Wilson, K. R. Oxidation of a Model Alkane Aerosol by Oh Radical: The Emergent Nature of Reactive Uptake. *Phys. Chem. Chem. Phys.* **2015**, *17*, 4412−4423.
(19) Wiegel, A. A.; Wilson, K. R.; Hinsberg, W. D.; Houle, F. A. Stochastic Methods for Aerosol Chemistry: A Compact Molecular Description of Functionalization and Fragmentation in the Heterogeneous Oxidation of Squalane Aerosol by Oh Radicals. *Phys. Chem. Chem. Phys.* **2015**, *17*, 4398−4411.
(20) Squadrito, G. L.; Postlethwait, E. M. On the Hydrophobicity of Nitrogen Dioxide: Could There Be a "Lens" Effect for No(2) Reaction Kinetics? *Nitric Oxide* **2009**, *21*, 104−109.
(21) Shaw, A. W.; Vosper, A. J. Solubility of Nitric Oxide in Aqueous and Nonaqueous Solvents. *J. Chem. Soc., Faraday Trans. 1* **1977**, *73*, 1239−1244.
(22) Goldstein, S.; Lind, J.; Merenyi, G. Reaction of Organic Peroxyl Radicals with •No2 and •No in Aqueous Solution: Intermediacy of Organic Peroxynitrate and Peroxynitrite Species. *J. Phys. Chem. A* **2004**, *108*, 1719−1725.
(23) Worton, D. R.; Isaacman, G.; Gentner, D. R.; Dallmann, T. R.; Chan, A. W. H.; Ruehl, C.; Kirchstetter, T. W.; Wilson, K. R.; Harley, R. A.; Goldstein, A. H. Lubricating Oil Dominates Primary Organic Aerosol Emissions from Motor Vehicles. *Environ. Sci. Technol.* **2014**, *48*, 3698−3706.
(24) Yeh, G. K.; Ziemann, P. J. Alkyl Nitrate Formation from the Reactions of C8−C14 N-Alkanes with Oh Radicals in the Presence of Nox: Measured Yields with Essential Corrections for Gas−Wall Partitioning. *J. Phys. Chem. A* **2014**, *118*, 8147−8157.
(25) Merényi, G.; Lind, J.; Goldstein, S.; Czapski, G. Mechanism and Thermochemistry of Peroxynitrite Decomposition in Water. *J. Phys. Chem. A* **1999**, *103*, 5685−5691.
(26) Hodzic, A.; Jimenez, J. L.; Madronich, S.; Canagaratna, M. R.; DeCarlo, P. F.; Kleinman, L.; Fast, J. Modeling Organic Aerosols in a Megacity: Potential Contribution of Semi-Volatile and Intermediate Volatility Primary Organic Compounds to Secondary Organic Aerosol Formation. *Atmos. Chem. Phys.* **2010**, *10*, 5491−5514.
(27) Dzepina, K.; Cappa, C. D.; Volkamer, R. M.; Madronich, S.; DeCarlo, P. F.; Zaveri, R. A.; Jimenez, J. L. Modeling the Multiday Evolution and Aging of Secondary Organic Aerosol During Milagro 2006. *Environ. Sci. Technol.* **2011**, *45*, 3496−3503.

DOI: 10.1021/acs.jpclett.5b02121
J. Phys. Chem. Lett. 2015, 6, 4451−4455